Revelation of the Nature of the Reducing Species in Titanocene Halide−Promoted Reductions

ARTICLE *in* JOURNAL OF THE AMERICAN CHEMICAL SOCIETY · JUNE 2004

Impact Factor: 12.11 · DOI: 10.1021/ja0491230 · Source: PubMed

J|A|C|S
ARTICLES
Published on Web 06/04/2004

Revelation of the Nature of the Reducing Species in Titanocene Halide-Promoted Reductions

Rasmus Juel Enemærke, Jens Larsen, Troels Skrydstrup,* and Kim Daasbjerg*

Contribution from the Department of Chemistry, University of Aarhus, Langelandsgade 140, 8000 Aarhus C, Denmark

Received February 17, 2004; E-mail: kdaa@chem.au.dk

Abstract: The fundamental nature of Ti^{III} complexes generated in tetrahydrofuran by reduction of Cp_2TiCl_2 has been clarified by means of cyclic voltammetry and kinetic measurements. While the electrochemical reduction of Cp_2TiCl_2 leads to the formation of $Cp_2TiCl_2^-$, the use of metals such as Zn, Al, or Mn as reductants affords Cp_2TiCl and $(Cp_2TiCl)_2$ in a mixture having a dimerization equilibrium constant of 3×10^3 M^{-1}, independent of the metal used. Thus, we find it unlikely that the trinuclear complexes or ionic clusters known from the solid phase should be present in solution as previously suggested. The standard potentials determined for the redox couples $Cp_2TiCl_2/Cp_2TiCl_2^-$, $(Cp_2TiCl)_2^+/(Cp_2TiCl)_2$, Cp_2TiCl^+/Cp_2TiCl, and Cp_2Ti^{2+}/Cp_2Ti^+ increase in the order listed. However, the reactivity of the different Ti^{III} complexes is assessed as $(Cp_2TiCl)_2 \gtrsim Cp_2TiCl \approx Cp_2Ti^+ \gg Cp_2TiCl_2^-$ in their reactions with benzyl chloride and benzaldehyde. None of the reactions proceed by an outer-sphere electron transfer pathway, and clearly the inner-sphere character is much higher in the case of Cp_2Ti^+ than for $(Cp_2TiCl)_2$, Cp_2TiCl, and in particular $Cp_2TiCl_2^-$. As to the electron acceptor, the inner-sphere character increases, going from benzyl chloride to benzaldehyde, and it is suggested that the chlorine atom in benzyl chloride and the oxygen atom in benzaldehyde may function as bridges between the reactants in the transition state.

Introduction

Low-valent metal complexes employed as single electron transferring agents are important reagents for promoting organic synthetic transformations.[1] One of these, which has become increasingly popular over the past few years, is bis(cyclopentadienyl)titanium chloride (Cp_2TiCl), promoting highly diastereoselective pinacol coupling reactions,[2] epoxide openings to alkyl radicals,[3] reductions of alkyl halides such as glycosyl bromides[4] and *vic*-dibromides,[5] Reformatsky additions,[6] and others.[7−9] The generation of the trivalent titanium species in tetrahydrofuran (THF) may be achieved by direct substitution of two of the chlorides in $TiCl_3$ with metalated cyclopentadiene[10] or by simple reduction of Cp_2TiCl_2 with metals such as zinc,[11] aluminum,[12] and manganese.[13] Cp_2TiCl has likewise been reported to be obtained after electrode reduction of Cp_2TiCl_2.[14] However, in our previous study concerning the electrode reduction of Cp_2TiX_2 (X = Cl, Br, and I), we showed that mixtures of $Cp_2TiX_2^-$, Cp_2TiX, and the dimer $(Cp_2TiX)_2$ are generated, with the former being the major species only in the case of X = Cl.[15]

The metal-based reductions have led to development of important reaction protocols catalytic with respect to the titanium complex, employing stoichiometric amounts of a metal reductant to regenerate the catalyst after electron transfer.[2c−i,3q−s,u,y,gg−ii,mm,vv,4f,8,9] Such applications significantly augment the utility of this reagent for organic synthesis, while justifying the development of more elaborate versions for asymmetric synthesis. Despite its synthetic importance, little is known about the mechanism of the electron transfers that it promotes to organic substrates. Information concerning the electronic interaction between the reductant and the substrate in the transition state would undoubtedly be of importance for understanding the reactivity of Ti^{III} reductants in addition to the development of new applications.

A complicating feature is the structure of the species produced from the above-described reduction of Cp_2TiCl_2 with metals. Previous reports have shown that trinuclear complexes (denoted **I** in Chart 1) may be isolated in the solid state, depending on the metal employed.[13,16] Such complexes have therefore been proposed to be the reducing species in solution accounting at the same time for the high *dl*-selectivities observed in pinacol couplings of aryl aldehydes in THF.[17] On the other hand, ESR and ENDOR studies of **I** prepared with zinc have provided evidence for the existence of a Ti^{III} cation in a frozen THF

(1) (a) Molander, G. A.; Harris, C. R. *Chem. Rev.* **1996**, *96*, 307. (b) Skrydstrup, T. *Angew. Chem., Int. Ed. Engl.* **1997**, *36*, 345. (c) Molander, G. A.; Harris, C. R. *Tetrahedron* **1998**, *54*, 3321. (d) Gansäuer, A. *Synlett* **1998**, 801. (e) Krief, A.; Laval, A.-M. *Chem. Rev.* **1999**, *99*, 745. (f) Gansäuer, A.; Bluhm, H. *Chem. Rev.* **2000**, *100*, 2771. (g) Spencer, R. P.; Schwartz, J. *Tetrahedron* **2000**, *56*, 2103. (h) Gansäuer, A. In *Radicals in Organic Synthesis*; Renaud, P., Sibi, M. P., Eds.; Wiley-VCH: Weinheim, Germany, 2001; Vol. 2, p 2007. (i) Li, J. J. *Tetrahedron* **2001**, *57*, 1. (j) Steel, P. G. *J. Chem. Soc., Perkin Trans. 1* **2001**, 2727.

(2) (a) Handa, Y.; Inanaga, J. *Tetrahedron Lett.* **1987**, *28*, 5717. (b) Barden, M. C.; Schwartz, J. *J. Am. Chem. Soc.* **1996**, *118*, 5484. (c) Gansäuer, A. *J. Chem. Soc., Chem. Commun.* **1997**, 457. (d) Gansäuer, A.; Moschioni, D.; Bauer, *Eur. J. Org. Chem.* **1998**, *1923*, 3. (e) Gansäuer, A.; Bauer, D. *J. Org. Chem.* **1998**, *63*, 2070. (f) Gansäuer, A.; Bauer, D. *Eur. J. Org. Chem.* **1998**, *2673*, 3. (g) Dunlap, M. S.; Nicholas, K. M. *Synth. Commun.* **1999**, *29*, 1097. (h) Halterman, R. L.; Zhu, C.; Chen, Z.; Dunlap, M. S.; Khan, M. A.; Nicholas, K. M. *Organometallics* **2000**, *19*, 3824. (i) Dunlap, M. S.; Nicholas, K. M. *J. Organomet. Chem.* **2001**, *630*, 125. (j) Lake, K.; Dorrell, M.; Blackman, N.; Khan, M. A.; Nicholas, K. M. *Organometallics* **2003**, *22*, 4260.

Chart 1. Proposed Structures of Reactive Trinuclear (**I**) and Dimeric (**II** and **III**) Complexes in THF

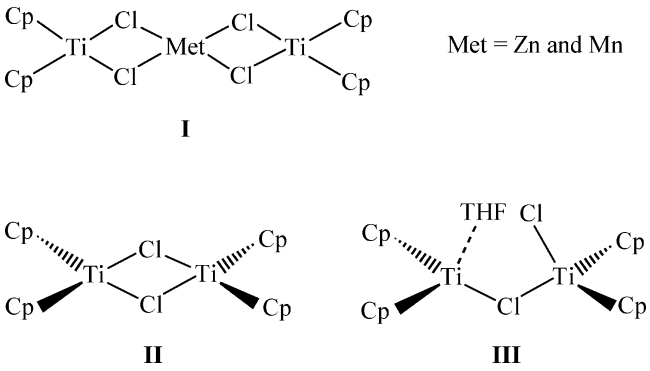

matrix.[18] Preliminary cyclic voltammetric studies also gave no indications of the presence of trinuclear complexes in solution.[19] Finally, a comparative study of the diastereoselectivities obtained in the pinacol coupling of benzaldehyde with metal-reduced Cp_2TiCl_2 and $(Cp_2TiCl)_2$ in the presence of trimethylsilyl chloride allowed Dunlap and Nicholas to propose the dimer to be the true reducing agent in THF.[2i]

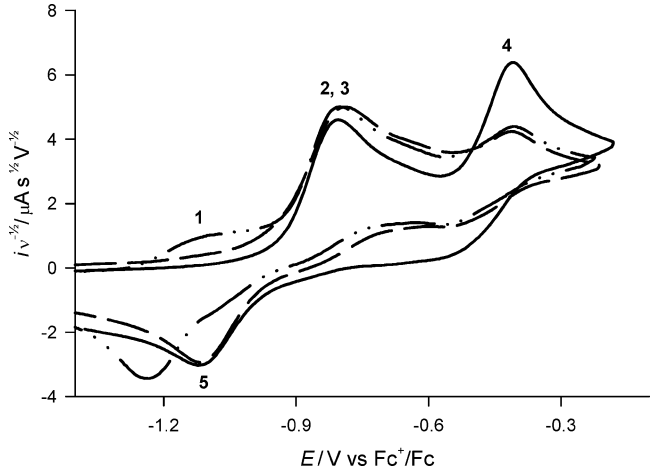

Figure 1. Cyclic voltammograms of 2 mM solutions of Zn−Cp_2TiCl_2 (—), Mn−Cp_2TiCl_2 (− − −), and Al−Cp_2TiCl_2 (− · · −) recorded at a sweep rate of 0.1 V s^{-1} in 0.2 M Bu_4NPF_6/THF.

Through a combination of kinetic and electrochemical investigations, we disclose in this article that trinuclear complexes **I** (or ionic clusters) *are not the reacting species in THF* despite their isolation and characterization in the solid phase and that common Ti^{III}-based reductants are formed in all cases, independent of the metal used. Our results substantiate the view that $(Cp_2TiCl)_2$ and Cp_2TiCl are the major reducing species in solution. In addition, we provide characterization of the electron-transferring abilities of Ti^{III} reductants with the two organic substrates, benzyl chloride and benzaldehyde, allowing further insight into the mechanism of the pertinent reduction processes.

Results and Discussions

Cyclic Voltammetry. Cyclic voltammetry studies of the three metal-reduced solutions of Cp_2TiCl_2 denoted Met−Cp_2TiCl_2 (Met = Zn, Mn, and Al) display a quite interesting picture as shown in Figure 1. All three voltammograms exhibit similar oxidation peaks at −0.8 (designated **2**/**3**) and −0.4 V (designated **4**) vs Fc^+/Fc (abbreviation for ferrocenium/ferrocene), respec-

(3) (a) Nugent, W. A.; RajanBabu, T. V. *J. Am. Chem. Soc.* **1988**, *110*, 8561. (b) RajanBabu, T. V.; Nugent, W. A. *J. Am. Chem. Soc.* **1989**, *111*, 4525. (c) RajanBabu, T. V.; Nugent, W. A.; Beattie, M. S. *J. Am. Chem. Soc.* **1990**, *112*, 6408. (d) Yadav, J. S.; Shekharam, T.; Gadgil, V. R. *J. Chem. Soc., Chem. Commun.* **1990**, 843. (e) Lowinger, T. B.; Weiler, L. *Can. J. Chem.* **1990**, *68*, 1636. (f) Merlic, C. A.; Xu, D. *J. Am. Chem. Soc.* **1991**, *113*, 9855. (g) Yadav, J. S.; Shekharam, T.; Srinivas, D. *Tetrahedron Lett.* **1992**, *33*, 7973. (h) Merlic, C. A.; Xu, D. *Tetrahedron Lett.* **1993**, *34*, 227. (i) RajanBabu, T. V.; Nugent, W. A. *J. Am. Chem. Soc.* **1994**, *116*, 986. (j) Golakoti, T.; Ogino, J.; Heltzel, C. E.; Husebo, T. L.; Jensen, C. M.; Larsen, L. K.; Petterson, G. M. L.; Moore, R. E.; Mooberry, S. L.; Corbett, T. H.; Valeriote, F. A. *J. Am. Chem. Soc.* **1995**, *117*, 12030. (k) Clive, D. L. J.; Magnusson, S. R. *Tetrahedron Lett.* **1995**, *36*, 15. (l) Clive, D. L. J.; Magnusson, S. R.; Manning, H. W.; Mayhew, D. L. *J. Org. Chem.* **1996**, *61*, 2095. (m) Maiti, G.; Roy, S. C. *J. Chem. Soc., Perkin Trans. 1* **1996**, 403. (n) Chakraborty, T. K.; Dutta, S. *J. Chem. Soc., Perkin Trans. 1* **1997**, 1257. (o) Weigand, S.; Brückner, R. *Synlett* **1997**, 225. (p) Yadav, J. S.; Srinivas, D. *Chem. Lett.* **1997**, 905. (q) Gansäuer, A.; Pierobon, M.; Bluhm, H. *Angew. Chem., Int. Ed.* **1998**, *37*, 101. (r) Gansäuer, A.; Bluhm, H. *J. Chem. Soc., Chem. Commun.* **1998**, 2143. (s) Gansäuer, A.; Bluhm, H.; Pierobon, M. *J. Am. Chem. Soc.* **1998**, *120*, 12849. (t) Mandal, P. K.; Maiti, G.; Roy, S. C. *J. Org. Chem.* **1998**, *63*, 2829. (u) Gansäuer, A.; Lauterbach, T.; Bluhm, H.; Noltemeyer, M. *Angew. Chem., Int. Ed.* **1999**, *38*, 2909. (v) Jørgensen, K. B.; Suenaga, T.; Nakata, T. *Tetrahedron Lett.* **1999**, *40*, 8855. (w) Mandel, P. K.; Maita, G. *Tetrahedron* **1999**, *55*, 11395. (x) Fernández-Mateos, A.; Martín de la Nava, E.; Coca, G. P.; Silvo, A. R.; González, R. R. *Org. Lett.* **1999**, *1*, 607. (y) Gansäuer, A.; Pierobon, M. *Synlett* **2000**, 1357. (z) Chakraborty, T. K.; Das, S. *Chem. Lett.* **2000**, 80. (aa) Rana, K. K.; Guin, C.; Roy, S. C. *Tetrahedron Lett.* **2000**, *41*, 9337. (bb) Dötz, K. H.; Gomes da Silva, E. *Tetrahedron* **2000**, *56*, 8291. (cc) Rana, K. K.; Guin, C.; Roy, S. C. *Synlett* **2001**, 1249. (dd) Barrero, A. F.; Cuerva, J. M.; Herrador, M. M.; Valdivia, M. V. *J. Org. Chem.* **2001**, *66*, 4074. (ee) Haruo, Y.; Hasegawa, T.; Tanaka, H.; Takahashi, T. *Synlett* **2001**, 1935. (ff) Nakai, K.; Kamoshita, M.; Doi, T.; Yamada, H.; Takahashi, T. *Tetrahedron Lett.* **2001**, *42*, 7855. (gg) Gansäuer, A.; Bluhm, H.; Pierobon, M.; Keller, M. *Organometallics* **2001**, *20*, 914. (hh) Gansäuer, A.; Pierobon, M.; Bluhm, H. *Synthesis* **2001**, 2500. (ii) Gansäuer, A.; Bluhm, H.; Lauterbach, T. *Adv. Synth. Catal.* **2001**, *343*, 785. (jj) Chakraborty, T. K.; Tapadar, S. *Tetrahedron Lett.* **2001**, *42*, 1375. (kk) Chakraborty, T. K.; Das, S.; Raju, T. V. *J. Org. Chem.* **2001**, *66*, 4091. (ll) Hardouin, C.; Chevallier, F.; Rousseau, B.; Doris, E. *J. Org. Chem.* **2001**, *66*, 1046. (mm) Gansäuer, A.; Rinker, B. *Tetrahedron* **2002**, *58*, 7017. (nn) Chakraborty, T. K.; Das, S. *Tetrahedron Lett.* **2002**, *43*, 2313. (oo) Parrish, J. D.; Little R. D. *Org. Lett.* **2002**, *4*, 1439. (pp) Barrero, A. F.; Oltra, J. E.; Cuerva, J. M.; Rosales, A. *J. Org. Chem.* **2002**, *67*, 2566. (qq) Rana, K. K.; Guin, C.; Roy, S. C. *J. Org. Chem.* **2002**, *67*, 3242. (rr) Hardouin, C.; Doris, E.; Rousseau, B.; Mioskowski, C. *Org. Lett.* **2002**, *4*, 1151. (ss) Hardouin, C.; Doris, E.; Rousseau, B.; Mioskowski, C. *J. Org. Chem.* **2002**, *67*, 6571. (tt) Barrero, A. F.; Cuerva, J. M.; Alvarez-Manzaneda, E. J.; Enrique Oltra, J.; Chahboun, R. *Tetrahedron Lett.* **2002**, *43*, 2793. (uu) Ruano, G.; Grande, M.; Anaya, J. *J. Org. Chem.* **2002**, *67*, 8243. (vv) Gansäuer, A.; Rinker, B.; Pierobon, M.; Grimme, S.; Gerenkamp, M.; Mück-Lichtenfeld, C. *Angew. Chem., Int. Ed.* **2003**, *42*, 3687. (ww) Anaya, J.; Fernández-Matos, A.; Grande, M.; Martiánez, J.; Ruano, G.; Rubio-González R. *Tetrahedron* **2003**, *59*, 241. (xx) Ruano, G.; Martiánez, J.; Grande, M.; Anaya, J. *J. Org. Chem.* **2003**, *68*, 2024. (yy) Barrero, A. F.; Rosales, A.; Cuerva, J. M.; Oltra, J. E. *Org. Lett.* **2003**, *5*, 1935.
(4) (a) Cavallaro, C. L.; Schwartz, J. *J. Org. Chem.* **1995**, *60*, 7055. (b) Spencer, R. P.; Schwartz, J. *Tetrahedron Lett.* **1996**, *37*, 4357. (c) Spencer, R. P.; Schwartz, J. *J. Org. Chem.* **1997**, *62*, 4204. (d) Spencer, R. P.; Cavallaro, C. L.; Schwartz, J. *J. Org. Chem.* **1999**, *64*, 3987. (e) Hansen, T.; Krintel, S. L.; Daasbjerg, K.; Skrydstrup, T. *Tetrahedron Lett.* **1999**, *40*, 6087. (f) Hansen, T.; Daasbjerg, K.; Skrydstrup, T. *Tetrahedron Lett.* **2000**, *41*, 8645.
(5) Davies, S. G.; Thomas, S. E. *Synthesis* **1984**, 1027.
(6) (a) Ding, Y.; Zhao, G. *J. Chem. Soc., Chem. Commun.* **1992**, 941. (b) Parrish, J. D.; Shelton, D. R.; Little, R. D. *Org. Lett.* **2003**, *5*, 3615.
(7) Russo, T.; Pinhas, A. R. *Organometallics* **1999**, *18*, 5344.
(8) Zhou, L.; Hirao, T. *Tetrahedron* **2001**, *57*, 6927.
(9) Barrero, A. F.; Rosales, A.; Cuerva, J. M.; Gansäuer, A.; Enrique Oltra, J. *Tetrahedron Lett.* **2003**, *44*, 1079.
(10) Manzer, L. E. *Inorganic Synthesis*; Wiley-Interscience, 1982; Vol. XXI, p 84.
(11) Coutts, R. S. P.; Wailes, P. C.; Martin, R. L. *J. Organomet. Chem.* **1973**, 375.
(12) Birmingham, J. M.; Fischer, A. K.; Wilkinson, G. *Naturwissenschaften* **1955**, *42*, 96.
(13) Sekutowski, D. J.; Stucky, G. D. *Inorg. Chem.* **1975**, *14*, 2192.
(14) (a) Mugnier, Y.; Moise, C.; Laviron, E. *J. Organomet. Chem.* **1981**, *204*, 61. (b) Mugnier, Y.; Moise, C.; Laviron, E. *Nouv. J. Chim.* **1982**, *6*, 197. (c) Mugnier, Y.; Fakhr, A.; Fauconet, M.; Moise, C.; Laviron, E. *Acta Chem. Scand.* **1983**, *B27*, 423. (d) Mugnier, Y.; Moise, C.; Laviron, E. *J. Organomet. Chem.* **1981**, *210*, 69. (e) Samuel, E.; Vedel, J. *Organometallics* **1989**, *8*, 237.
(15) Enemærke, R. J.; Larsen, J.; Skrydstrup, T.; Daasbjerg, K. *Organometallics* **2004**, *23*, 1866.
(16) Sekutowski, D.; Jungst, R.; Stucky, G. D. *Inorg. Chem.* **1978**, *17*, 1848.
(17) For a discussion of trinuclear complexes in solution, see ref 1d and references therein.
(18) Gourier, D.; Vivien, D.; Samuel, E. *J. Am. Chem. Soc.* **1985**, *107*, 7418.
(19) Enemærke, R. J.; Hjøllund, G. H.; Daasbjerg, K.; Skrydstrup, T. *C. R. Acad. Sci.* **2001**, *4*, 435.

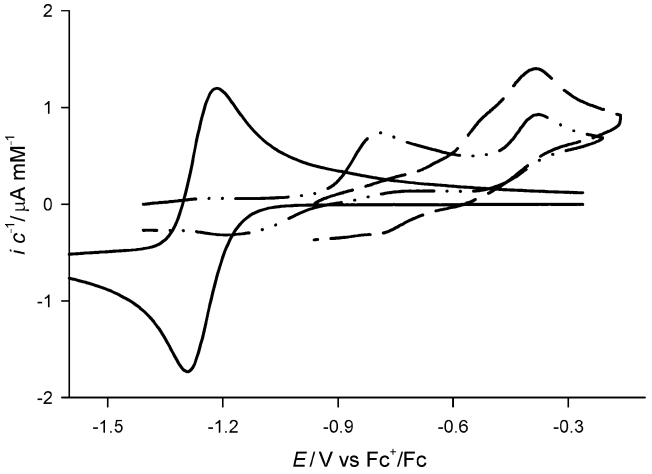

Figure 2. Cyclic voltammograms of 1.0 mM Cp_2TiCl_2 (—), 0.4 mM Cp_2Ti^+ (– – –), and 1.5 mM $Cp_2TiCl/(Cp_2TiCl)_2$ (– • • –) recorded at a sweep rate of 0.1 V s^{-1} in 0.2 M Bu_4NPF_6/THF. Currents are normalized with respect to concentration to facilitate comparison.

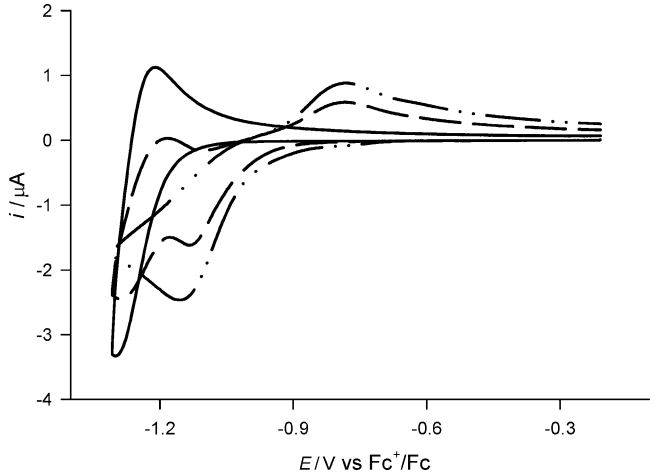

Figure 3. Cyclic voltammograms of 2 mM Cp_2TiCl_2 in the presence of 0 (—), 0.5 (– – –), and 1 equiv $ZnCl_2$ (– • • –) recorded at a sweep rate of 0.1 V s^{-1} in 0.2 M Bu_4NPF_6/THF. The sweep could not be extended past −1.3 V in the negative direction because of the deleterious adsorption of $ZnCl_2$.

tively, while an additional peak is observed at −1.1 V vs Fc$^+$/Fc (designated **1**) in the case of Met = Al. As described below, the broad **2**/**3** peak actually originates from two oxidation processes. On the reverse sweep a reduction peak (designated **5**) appears at ca. −1.2 V vs Fc$^+$/Fc, being slightly dependent on which metal considered. The fact that the peak potentials for the three different metal-reduced solutions are the same indicates that the waves originate from identical species and that trinuclear complexes are unlikely to be present in any of these solutions. Clearly, the oxidation potential of **I** (see Chart 1) would be expected to differ for the different metals.

The most likely candidates as common Ti^{III}-based species are $Cp_2TiCl_2^-$, $(Cp_2TiCl)_2$, Cp_2TiCl, and Cp_2Ti^+. The structure of the $(Cp_2TiCl)_2$ dimer well-characterized from the solid state[11] is shown as **II** in Chart 1, while **III** presents a tentative suggestion for its structure in THF as discussed below. Fortunately, all of these species can be generated either separately or as a mixture (see the Experimental Section).[15] In Figure 2, we have collected cyclic voltammograms of Cp_2TiCl_2, $Cp_2Ti^+PF_6^-$, and the mixture $Cp_2TiCl/(Cp_2TiCl)_2$ (denoted "Cp_2TiCl" in ref 15) to be able to compare their characteristics with those of the voltammograms of Met−Cp_2TiCl_2 in Figure 1. In accordance with expectation, $Cp_2TiCl_2^-$ with an oxidation peak potential of −1.2 V vs Fc$^+$/Fc is found to be the easiest one to oxidize, whereas Cp_2Ti^+ with a potential of −0.4 V vs Fc$^+$/Fc is the most difficult one. Both $(Cp_2TiCl)_2$ and Cp_2TiCl show intermediate behavior, having essentially the same oxidation peak potentials of −0.8 V vs Fc$^+$/Fc; the appearance of the additional peak at −0.4 V vs Fc$^+$/Fc in this case is due to the generation of Cp_2Ti^+ during the cyclic voltammetric sweep.[15] The nice correspondence of these peaks with those recorded for the metal-generated solutions strongly suggests that the origin of peaks **1**−**5** can be ascribed to the electrode processes depicted in eqs 1−4.

$$\mathbf{1/5}:\ Cp_2TiCl_2^- - e \rightleftarrows Cp_2TiCl_2 \qquad (1)$$

$$\mathbf{2}:\ (Cp_2TiCl)_2 - e \rightleftarrows (Cp_2TiCl)_2^+ \qquad (2)$$

$$\mathbf{3}:\ Cp_2TiCl - e \rightleftarrows Cp_2TiCl^+ \qquad (3)$$

$$\mathbf{4}:\ Cp_2Ti^+ - e \rightleftarrows Cp_2Ti^{2+} \qquad (4)$$

It should be emphasized that because cyclic voltammetry is a dynamic technique, the species detected are not necessarily present initially in the solution but may simply be generated during the sweep. This also provides the explanation why the oxidation wave pertaining to Cp_2Ti^+ appears in the voltammogram of $Cp_2TiCl/(Cp_2TiCl)_2$. Thus, one cannot a priori conclude that all four Ti^{III}-based molecules are present in the metal-generated solutions. Indeed, we will show below on the basis of an extended analysis involving both cyclic voltammetry and kinetic measurements that the two principal Ti^{III} species are the dimer, $(Cp_2TiCl)_2$, in equilibrium with its monomer, Cp_2TiCl, and that the following reactions apply in the description of the metal-based reductions of Cp_2TiCl_2.

$$Zn + 2Cp_2TiCl_2 \rightarrow ZnCl_2 + 2Cp_2TiCl \qquad (5)$$

$$Mn + 2Cp_2TiCl_2 \rightarrow MnCl_2 + 2Cp_2TiCl \qquad (6)$$

$$Al + 3Cp_2TiCl_2 \rightarrow AlCl_3 + 3Cp_2TiCl \qquad (7)$$

$$2Cp_2TiCl \underset{k_{-8}}{\overset{k_8}{\rightleftharpoons}} (Cp_2TiCl)_2 \qquad (8)$$

One of the prominent features of the Met−Cp_2TiCl_2 solutions is the presence of metal chlorides and their possible involvement in chloride transfer reactions. This explains why the **1**/**5** peaks of the $Cp_2TiCl_2/Cp_2TiCl_2^-$ redox couple in the metal-generated cases are not completely coincident with those obtained for an authentic sample of Cp_2TiCl_2. As seen in Figure 3, the peaks recorded for Cp_2TiCl_2 are gradually shifted upon addition of $ZnCl_2$ to come in closer agreement with those recorded for Zn−Cp_2TiCl_2. At the same time, this is also the origin of the variation in the relative currents of the oxidation waves for the different Met−Cp_2TiCl_2 solutions. Without doubt, the chloride abstraction proceeds with greater ease from $AlCl_3$ than from $ZnCl_2$ and $MnCl_2$ since peak **1** attributed to the oxidation of $Cp_2TiCl_2^-$ can only be observed in the former case (see Figure 1). The relative importance of this peak increases upon lowering the sweep rate. Moreover, addition of excess Bu_4NCl to any of the solutions results in the transformation of $(Cp_2TiCl)_2$, Cp_2TiCl and Cp_2Ti^+ to $Cp_2TiCl_2^-$ as shown in Figure 4.

To substantiate the working hypothesis that $(Cp_2TiCl)_2$ and Cp_2TiCl should be the principal Ti^{III} species present in the

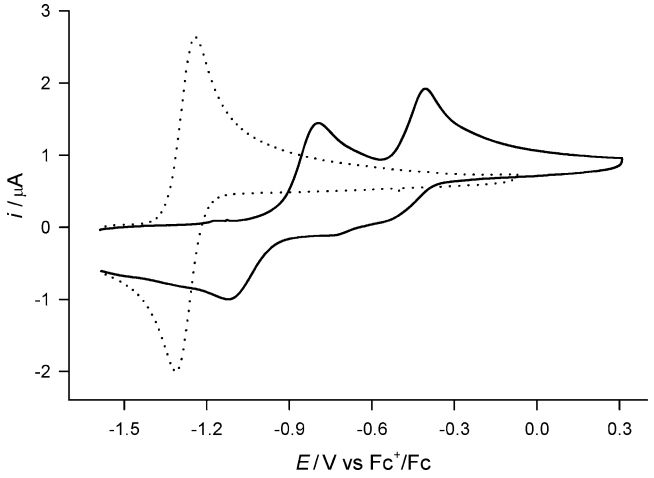

Figure 4. Cyclic voltammograms of 2 mM $Zn-Cp_2TiCl_2$ in the absence (—) and presence (•••) of 20 mM Bu_4NCl recorded at a sweep rate of 0.1 V s^{-1} in 0.2 M Bu_4NPF_6/THF.

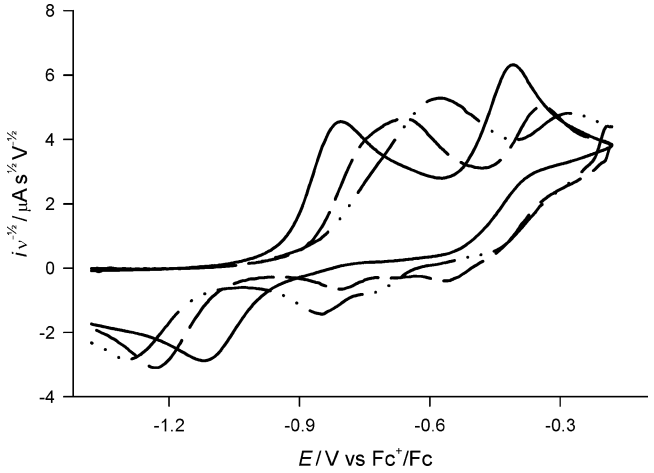

Figure 5. Cyclic voltammograms of 2 mM solutions of $Zn-Cp_2TiCl_2$ recorded at sweep rates of 0.1 (—), 10 (– – –), and 50 V s^{-1} (– • • –) in 0.2 M Bu_4NPF_6/THF. Currents are normalized with respect to sweep rate.

$Met-Cp_2TiCl_2$ solutions, a detailed cyclic voltammetric analysis was carried out. The first important observation is that the relative current of the Cp_2Ti^+ oxidation wave **4** decreases with increasing sweep rate as illustrated in the case of $Zn-Cp_2TiCl_2$ in Figure 5. At the same time, the number of electrons involved in the **2**/**3** wave goes from $^1/_2$ toward 1. Experiments carried out at a sweep rate of 1 kV s^{-1} at a 10 μm glassy carbon ultramicroelectrode confirm this tendency as wave **4** essentially disappears. Thus, it is concluded that Cp_2Ti^+ is not present in any of the $Met-Cp_2TiCl_2$ solutions initially but that it is generated at the electrode surface as a consequence of chemical reactions occurring during the sweep. In a previous electrochemical study on metal-free Ti^{III}-based solutions, Laviron et al.[14d] suggested that Cp_2Ti^+ is formed in a fast father–son reaction (eq 9) involving chloride transfer from Cp_2TiCl to Cp_2TiCl^+, with the latter being formed in the electrode process of eq 3.

$$Cp_2TiCl + Cp_2TiCl^+ \underset{k_{-9}}{\overset{k_9}{\rightleftharpoons}} Cp_2Ti^+ + Cp_2TiCl_2 \qquad (9)$$

Indeed, the concomitant generation of Cp_2TiCl_2 in eq 9 is detectable on the reverse sweep (see Figure 1). However, in the present case one should also take into account that the formation of Cp_2TiCl_2 may occur through competing chloride transfers to Cp_2TiCl^+ from the metal chlorides generated in eqs 5–7.

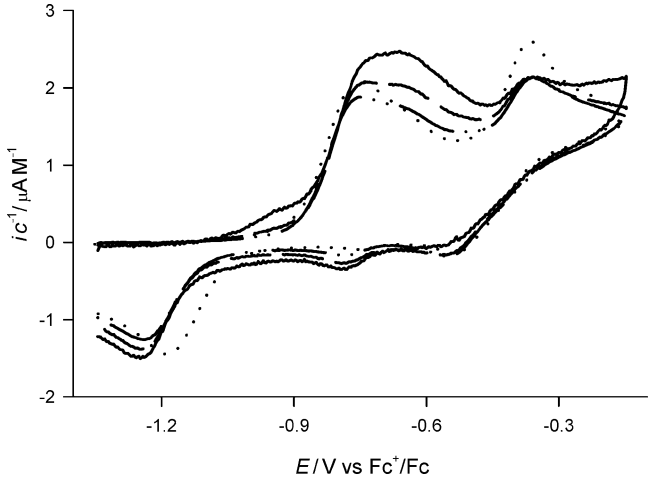

Figure 6. Cyclic voltammograms of solutions containing $Zn-Cp_2TiCl_2$ in concentrations of 0.2 (—), 0.4 (– – –), 1 (– • • –), and 2 mM (•••) recorded at a sweep rate of 1 V s^{-1} in 0.2 M Bu_4NPF_6/THF. Currents are normalized with respect to concentration.

The evidence for the existence of the equilibrium reaction, eq 8, involving Cp_2TiCl and $(Cp_2TiCl)_2$ is provided by voltammograms recorded for $Zn-Cp_2TiCl_2$ at various concentrations. As seen in Figure 6, the broad wave appearing at −0.8 V vs Fc^+/Fc consists of two processes, with the first one becoming more dominant as the concentration increases. Thus, the first peak **2** is attributed to the oxidation of the dimer, eq 2, and the second peak **3** to the oxidation of the monomer, eq 3, with the relative height being affected by the presence of the equilibrium reaction in eq 8. Assignment of the broad wave to the oxidation of trinuclear complexes is ruled out by the fact that exactly the same type of splitting is observed for $Al-Cp_2TiCl_2$ and $Mn-Cp_2TiCl_2$ as well as the metal-free $Cp_2TiCl/(Cp_2TiCl)_2$ solution analyzed previously (see Figure 2).[15]

Another interesting point is that eqs 3 and 9 involving the oxidation of Cp_2TiCl followed by the father–son reaction cannot be the only pathway for the generation of Cp_2Ti^+ during the cyclic voltammetric sweep. Peak **4** is also apparent at high concentrations and low sweep rates, although the oxidation goes almost exclusively through $(Cp_2TiCl)_2$ in eq 2 under such conditions. This implies that Cp_2Ti^+ may originate from the fragmentation of $(Cp_2TiCl)_2^+$ as well. On account of the observations that the reduction of Cp_2TiCl_2 is detectable on the reverse sweep and that the peak current ratio for the oxidation waves **2** and **4** approaches unity at high concentrations and low sweep rates, the fragmentation is proposed to follow the pathway in eq 10.

$$(Cp_2TiCl)_2^+ \underset{k_{-10}}{\overset{k_{10}}{\rightleftharpoons}} Cp_2Ti^+ + Cp_2TiCl_2 \qquad (10)$$

Competing chloride transfers from the metal chlorides to $(Cp_2TiCl)_2^+$ are found to be slower processes and thus not considered further (see the Supporting Information).

On the basis of the above information, we propose that a common reaction scheme, a so-called mesh scheme,[20] can be set up for the three $Met-Cp_2TiCl_2$ systems (Scheme 1).

Scheme 1. Mesh Scheme Describing the Reaction Mechanism for the Electrode Reactions of Met−Cp_2TiCl_2 (Met = Zn, Mn, or Al) in THF

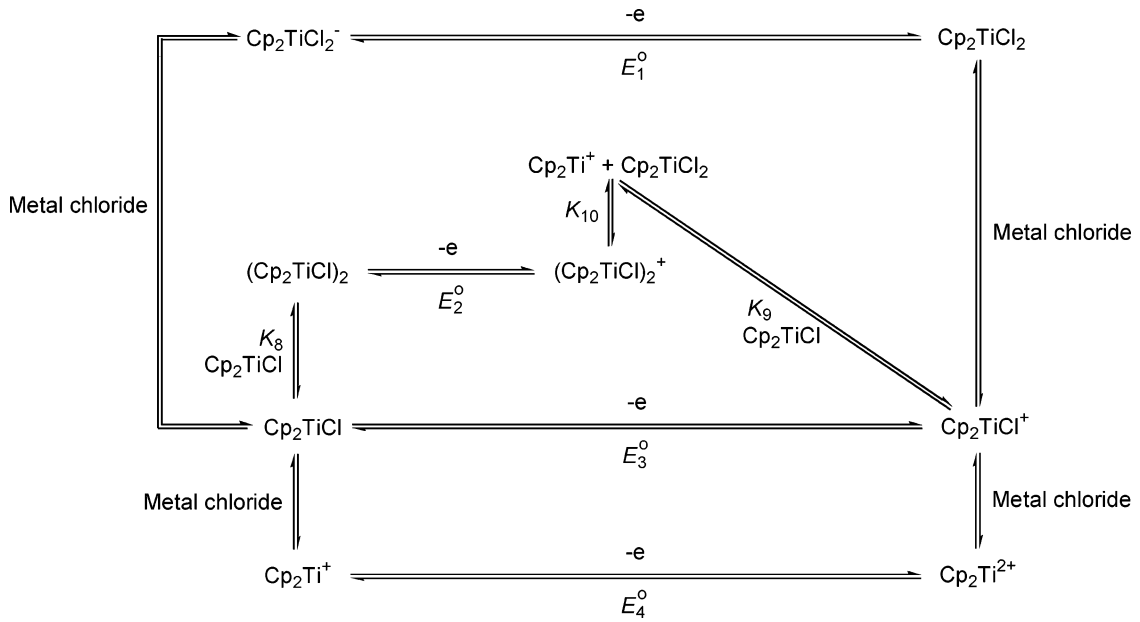

In the Supporting Information, detailed versions of this scheme are provided for each metal. The mesh scheme incorporates the four relevant electrochemical processes, eqs 1−4, along with a number of chemical reactions, including eqs 8−10. Among the latter, eq 8 is a key reaction because the equilibrium constant, K_8, determines the actual composition of the solution while the associated rate constants are essential parameters for describing the compositional changes occurring at the electrode surface during a chemical or electrochemical reaction. The oxidation of both Cp_2TiCl and $(Cp_2TiCl)_2$ leads ultimately to the formation of Cp_2Ti^+ and Cp_2TiCl_2. As no peak corresponding to the reduction of Cp_2TiCl^+ can be monitored in the cyclic voltammograms, even at high sweep rates, it is proposed that Cp_2TiCl^+ reacts rapidly with Cp_2TiCl or in particular metal chlorides to yield Cp_2TiCl_2. Likewise, the absence at low sweep rates of a cyclic voltammetric reduction wave pertaining to Cp_2Ti^{2+} formed upon oxidation of Cp_2Ti^+ in eq 4 suggests that Cp_2Ti^{2+} will abstract chloride from the metal chlorides. On the other hand, the lack of peak **1** in double sweep experiments for Met = Zn and Mn indicates that the chloride transfer reactions may go the other way around too, i.e., the metal chlorides can abstract chloride effectively from $Cp_2TiCl_2^-$ produced upon the electrochemical reduction of Cp_2TiCl_2 in eq 1. In general, Ti^{IV}- but not Ti^{III}-based species thus are capable of abstracting chloride from the metal chlorides with the Al−Cp_2TiCl_2 system presenting a notable exception, as peak **1** in this case is observable.

From a mechanistic point of view it is crucial to determine the exact composition of the solutions. Unfortunately, voltammograms recorded at low sweep rates will be influenced strongly by the chemical reactions preceding or following the electrode processes. For instance, the overall oxidation of the relatively facile $Cp_2TiCl/(Cp_2TiCl)_2$ equilibrium system will mainly go through the dimer under such conditions, as this is the species most easily oxidized. In principle, it should be possible to outrun all chemical reactions by applying high sweep rates. However, in the present study we found that the largest applicable value for quantitative purposes was about 50 V s^{-1}; at higher sweep rates the **2** and **3** waves broadened and merged, preventing us from measuring the equilibrium constant of eq 8 directly. Other techniques such as chronoamperometry and sampled current voltammetry were considered as well,[21] but they did not provide information that was not obtainable by cyclic voltammetry.

All relevant potentials, heterogeneous and homogeneous rate constants, and equilibrium constants have been extracted by digital simulations (using the program DigiSim 3.03)[22] of experimentally obtained voltammograms recorded at different sweep rates of 0.1−50 V s^{-1} and concentrations of 0.17−2.0 mM. For these kinds of measurements, it is important that the number of experimental observations is large to diminish the overall uncertainty. In addition, the whole collection of voltammograms recorded for each solution of Met−Cp_2TiCl_2 has been simulated simultaneously to obtain the most consistent set of results. The main emphasis in the simulation procedure has been to reproduce the relative currents and the peak potentials with less attention paid to the shape of the relatively broad curves. As described in the Supporting Information, the procedure is based partly on a subjective judgment of which values make the better fits because of the large number of variables present.

The adjustable parameters in the simulation procedure include standard potentials, equilibrium constants, homogeneous and heterogeneous rate constants, symmetry factors, and diffusion coefficients. Of these, the last two are considered to be of less importance, and thus they are kept fixed. The values of the standard potentials, $E°$, and the heterogeneous rate constants, k_s, are very important for the quality of the fits, as they essentially determine the position of the peaks. For k_s we find relatively small values less than 0.1 cm s^{-1}; therefore, the

(20) Usually the presence of at least three redox states as well as chemical states would be required for describing such a mechanism by a mesh scheme. Thus, in the present case one might argue that the mechanistic scheme is of the ladder type, if the $(Cp_2TiCl)_2^+$ species with its combination of Ti^{III} and Ti^{IV} atoms is not considered as representing a distinct redox state (see also: Evans, D. H. *Chem. Rev.* **1990**, *90*, 739).

(21) Amatore, C.; Jutand, A.; Khalil, F.; M'Barki, M. A.; Mottier, L. *Organometallics* **1993**, *12*, 3168.

(22) Rudolph, M.; Feldberg, S. W. *DigiSim*, version 3.03; Bioanalytical Systems, Inc.: West Lafayette, IN.

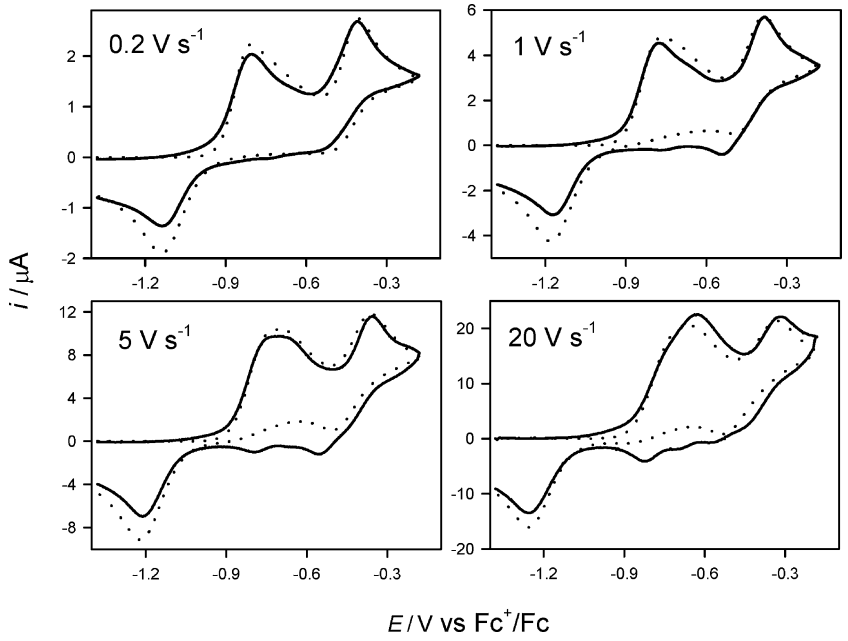

Figure 7. Recorded (−) and simulated (···) cyclic voltammograms of 2 mM Zn−Cp_2TiCl_2 at sweep rates of 0.2, 1, 5, and 20 V s^{-1} in 0.2 M Bu_4NPF_6/THF. The simulation parameters employed can be found in Table 1 and in the Supporting Information.

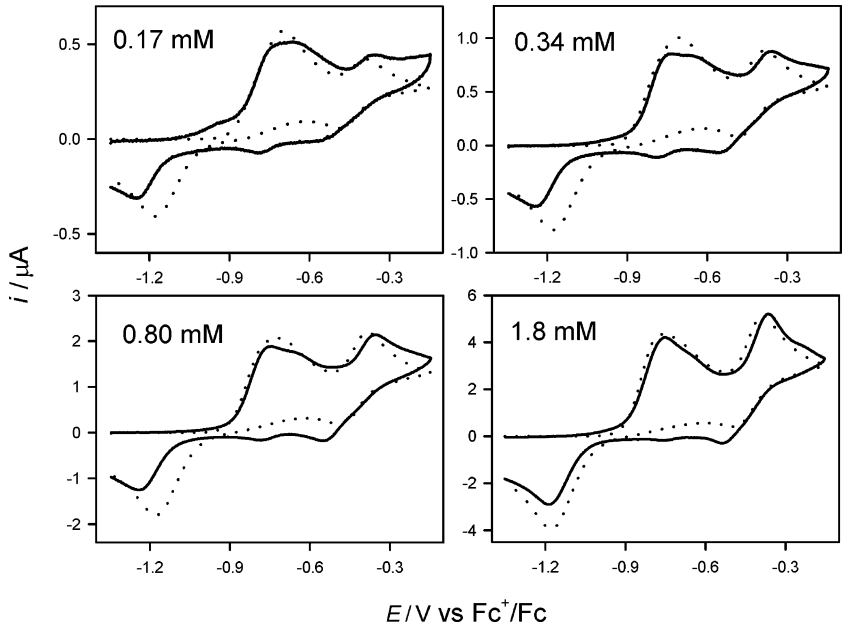

Figure 8. Recorded (−) and simulated (···) cyclic voltammograms of Zn−Cp_2TiCl_2 in concentrations of 0.17, 0.34, 0.80, and 1.80 mM at a sweep rate of 1 V s^{-1} in 0.2 M Bu_4NPF_6/THF. The simulation parameters employed can be found in Table 1 and in the Supporting Information.

electrode processes can be considered to be quasireversible for most of the sweep rates employed. Thus, the influence on the peak potentials from homogeneous follow-up or preceding reactions is not as pronounced as if the electrode processes had been reversible. On the other hand, the homogeneous kinetics in terms of the rate constants involved exerts a large influence on the peak currents and the wave pattern.

The fits are acceptable as illustrated in Figures 7 and 8 for Zn−Cp_2TiCl_2. In general, the oxidative sweep is described more successfully than the reductive one, as the simulations seem to overestimate somewhat the reduction wave of Cp_2TiCl_2. This indicates that the products formed during the oxidative sweep are not all transformed to Cp_2TiCl_2 as assumed in the simulations, but that some of them disappear through other routes. Indeed, it is likely as discussed elsewhere[15] that a side reaction between Cp_2Ti^{2+} and the solvent, THF, may take place. The latter reaction was not incorporated in the simulations as its effect on the determination of the other parameters in any case would be small. The simulations also showed that the father−son reaction involving Cp_2TiCl^+ in eq 9 will be outrun by chloride transfer reactions, and accordingly, k_9 was set equal to the upper limit of 5×10^3 M^{-1} s^{-1} found previously for the $Cp_2TiCl/(Cp_2TiCl)_2$ case.[15] A detailed description of the exact model parameters used and a compilation of relevant fits can be found in the Supporting Information.

The essential data extracted from the simulation procedure are collected in Table 1. Note that all potentials listed are referenced against Fc^+/Fc, but they can easily be converted to

Table 1. Relevant Data Extracted from Cyclic Voltammograms Recorded on Met−Cp_2TiCl_2 Solutions[a]

	Zn–Cp_2TiCl_2	Mn–Cp_2TiCl_2	Al–Cp_2TiCl_2	$Cp_2TiCl/(Cp_2TiCl)_2$[b]
E°_1/V vs Fc^+/Fc [c]	−1.20 ± 0.03	−1.20 ± 0.03	−1.24 ± 0.03	−1.27 ± 0.04
E°_2/V vs Fc^+/Fc [c]	−0.81 ± 0.03	−0.82 ± 0.03	−0.82 ± 0.03	−0.81 ± 0.02
E°_3/V vs Fc^+/Fc [c]	−0.75 ± 0.03	−0.77 ± 0.03	−0.76 ± 0.03	−0.75 ± 0.01
E°_4/V vs Fc^+/Fc [c]	−0.43 ± 0.03	−0.43 ± 0.03	−0.43 ± 0.03	−0.41 ± 0.02
$k_{s,1}$/cm s^{-1}	0.04	0.04	0.04	0.04
$k_{s,2}$/cm s^{-1}	0.02	0.02	0.02	0.02
$k_{s,3}$/cm s^{-1}	0.008	0.008	0.008	0.008
$k_{s,4}$/cm s^{-1}	0.015	0.015	0.015	0.015
K_8/ M^{-1}	3 (2−5) × 10^3	3 (2−5) × 10^3	3 (2−5) × 10^3	3 (2−7) × 10^3
k_8/ M^{-1} s^{-1}	2 (1−10) × 10^4	1 (0.5−5) × 10^5	5 (2−10) × 10^5	2 (0.5−4) × 10^4
k_{-8}/s^{-1}	6.7 (2−50)	33 (10−250)	167 (50−1000)	6.7 (2−17)
K_9/M^{-1}[d]	3.2 × 10^7	2.2 × 10^7	3.2 × 10^7	3.2 × 10^7
k_9/$M^{-1}s^{-1}$	<5 × 10^3[e]	<5 × 10^3[e]	< 5 × 10^3[e]	<5 × 10^3[f]
k_{-9}/s^{-1}	<1.6 × 10^{-4}[e]	<2.3 × 10^{-4}[e]	< 1.6 × 10^{-4}[e]	<1.6 × 10^{-4}[f]
K_{10}/M	1 (0.01−10^5) × 10^3	1 (0.01−10^5) × 10^3	1 (0.5−1.5) × 10^3[g]	1 (0.01−10^5) ×10^3
k_{10}/s^{-1}	3 (1−50) × 10^2	3 (1−50) × 10^2	3 (2−5) × 10^2[g]	1 (0.1−5) × 10^2
k_{-10}/ M^{-1} s^{-1}	0.3 (10^{-5}−30)	0.3 (10^{-5}−30)	0.3 (0.13−1)[g]	0.1 (10^{-5}−50)

[a] The tabulated values are the ones providing the best fits, while those given in parentheses describe the intervals of tolerance, as determined from a manual adjustment of the parameters. To minimize the number of adjustable parameters, the uncertainties on the k_s values were not determined, but in general they can be assumed to be on the order of 50%. [b] The results for $Cp_2TiCl/(Cp_2TiCl)_2$ are taken from ref 15 (denoted "Cp_2TiCl" therein). [c] Standard potentials are defined as reduction potentials and can be converted to SCE by adding 0.52 V. [d] Calculated automatically by the DigiSim program from a thermochemical cycle. [e] The simulations are found to be largely unaffected by the exact value of k_9, and accordingly the latter is set equal to the upper limit determined for the $Cp_2TiCl/(Cp_2TiCl)_2$ system. [f] An upper limit can be determined from simulations; see ref 15. [g] The simulations are found to be very sensitive toward changes in these parameters because of the reversible reactions occurring between aluminum chloride and the different titanium-based species.

SCE by adding 0.52 V.[23] On the basis of a simple comparison of the potential values that exhibit a variation of as much as 0.8 V, the electron-donating abilities of the different Ti^{III}-based species should be in the order $Cp_2TiCl_2^- \gg (Cp_2TiCl)_2 > Cp_2TiCl \gg Cp_2Ti^+$ from a thermodynamic point of view. However, such a consideration does not take into account that the reactivity of an electron donor is dependent on other factors as well, such as self-exchange reorganization energies, electrostatic work terms, and last but not least, inner-sphere character of the transition state. In fact, the determination of heterogeneous rate constants in the range of 0.008−0.04 cm s^{-1} for all four species would suggest that the pertinent self-exchange reorganization energies are relatively large.[24] Usually this would imply large intrinsic barriers and thus kinetically slow electron-transfer processes, unless there are favorable interactions present between the donor and acceptor in the transition state.

According to the equilibrium data, the dominant species in all Met−Cp_2TiCl_2 solutions are Cp_2TiCl and $(Cp_2TiCl)_2$ while there will be contribution from neither Cp_2Ti^+ nor $Cp_2TiCl_2^-$. It should be noted that the latter is the major species generated in the electrochemical reduction of Cp_2TiCl_2.[15] The value of 3 × 10^3 M^{-1} found for the equilibrium constant K_8 is independent of the metal considered. Actually, it is even equal to that obtained for a metal-free solution,[15] showing that the metal chlorides exert no influence on the position of the dimerization equilibrium, although the associated rate constants k_8 and k_{-8} both increase by a factor of 25 going from Met = Zn to Al. As to the composition of Met−Cp_2TiCl_2 solutions, the distribution of Ti^{III} species in a 0.5 mM solution, for example, will be 0.22 mM Cp_2TiCl and 0.14 mM $(Cp_2TiCl)_2$, while the corresponding numbers for a 100 mM solution will be 4 and 48 mM. Depending on the exact reaction conditions (catalytic or stoichiometric),[1−9] either of the two species may thus be the dominant one. In our previous study we showed that $Cp_2TiCl_2^-$ could be generated from Cp_2TiCl and free Cl^- with a relatively large formation equilibrium constant of 10^4 M^{-1}.[15] Still, $Cp_2TiCl_2^-$ will not be present in the Met−Cp_2TiCl_2 solutions, as chloride is firmly bound in the corresponding metal chlorides. Only in the case of Al−Cp_2TiCl_2 is the chloride transfer from $AlCl_3$ sufficiently fast (see the Supporting Information) to ensure production of detectable amounts of $Cp_2TiCl_2^-$ during a cyclic voltammetric sweep. On the other hand, $Cp_2TiCl_2^-$ can easily be made the principal Ti^{III} species in any of the solutions, if Bu_4NCl is added. The structure of the oxidized dimer $(Cp_2TiCl)_2^+$ is relatively fragile, endowed by a rate constant k_{10} of 300 s^{-1} for its fragmentation. As shown in our previous study, the latter process can be further accelerated by the presence of a nucleophile such as chloride.[15]

Kinetic Studies. With the aim of characterizing the reactivity and electron-donating abilities of the different Ti^{III}-based reductants, $Cp_2TiCl_2^-$, $(Cp_2TiCl)_2$, Cp_2TiCl, and Cp_2Ti^+, kinetic studies were carried out on their reactions with benzyl chloride (BnCl) and benzaldehyde (PhCHO). A description of the experiments involving $Cp_2TiCl_2^-$ and BnCl is provided elsewhere.[15] The measurements were performed by following the overall absorption decay of the Ti^{III} species and/or the equivalent buildup of Ti^{IV} species using excess of substrate.

Benzyl Chloride. The fact that the Met−Cp_2TiCl_2 solutions are mixtures of Cp_2TiCl and $(Cp_2TiCl)_2$ complicates the kinetic analysis in the sense that their reactivities have to be studied through a variation of the equilibrium concentrations. According to eq 8 the larger the overall concentration of Met−Cp_2TiCl_2 becomes, the more dominant the dimer will be. In Figure 9, we have collected kinetic traces for the buildup of Ti^{IV} using three different concentrations of Zn−Cp_2TiCl_2 in the presence of excess BnCl. The development is distinct in the sense that the overall kinetics becomes slower as the concentration is raised because of the influence from the equilibrium reaction in eq 8. The same behavior is seen for the two other Met−Cp_2TiCl_2 solutions.

(23) Enemærke, R. J.; Daasbjerg, K.; Skrydstrup, T. *J. Chem. Soc., Chem. Commun.* **1999**, 343.
(24) Enemærke, R. J.; Hertz, T.; Skrydstrup, T.; Daasbjerg, K. *Chem. Eur. J.* **2000**, *6*, 3747.

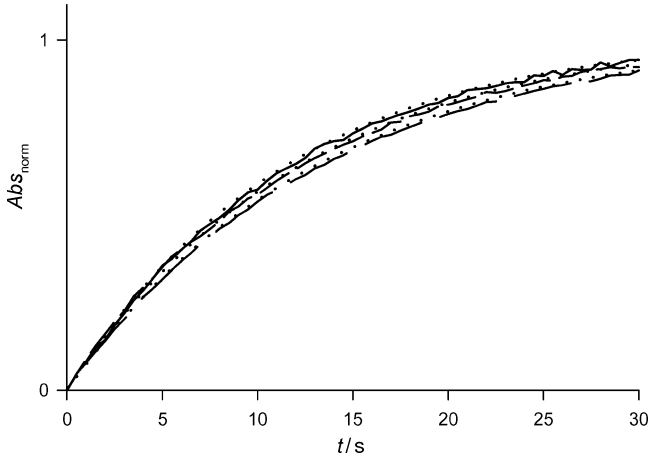

Figure 9. Kinetic traces recorded for the buildup of Ti^{IV} at $\lambda = 535$ nm in THF for the reactions of 87 mM BnCl with 0.8 (—), 1.8 (– – –), and 4.4 mM (— — —) solutions of $Zn-Cp_2TiCl_2$. Absorbances are normalized (using final absorbance = 1) to facilitate comparison. The dotted curves are the best fits based on simulation of eqs 8 and 11−15, providing $k_{11} = 0.66\ M^{-1}\ s^{-1}$ and $k_{13} = 0.80\ M^{-1}\ s^{-1}$.

The mechanistic basis for carrying out the fitting procedure consists of eq 8 along with eqs 11−15, involving both Cp_2TiCl and $(Cp_2TiCl)_2$ as reactive species.

$$Cp_2TiCl + BnCl \xrightarrow{k_{11}} [Cp_2TiCl^+ + Cl^- + Bn^\bullet] \rightarrow Cp_2TiCl_2 + Bn^\bullet \quad (11)$$

$$Cp_2TiCl + Bn^\bullet \rightarrow [Cp_2TiCl^+ + Bn^-] \rightarrow Cp_2TiClBn \quad (12)$$

$$(Cp_2TiCl)_2 + BnCl \xrightarrow{k_{13}} [(Cp_2TiCl)_2^+ + Cl^- + Bn^\bullet] \rightarrow Cp_2TiCl + Cp_2TiCl_2 + Bn^\bullet \quad (13)$$

$$(Cp_2TiCl)_2 + Bn^\bullet \rightarrow [(Cp_2TiCl)_2^+ + Bn^-] \rightarrow Cp_2TiCl + Cp_2TiClBn \quad (14)$$

$$Cp_2TiClBn + BnCl \rightarrow Cp_2TiCl_2 + Bn_2 \quad (15)$$

The hypothesis is that in the actual electron-transfer step between Cp_2TiCl and BnCl depicted in eq 11, the benzyl radical, $Bn^\bullet$, is formed along with chloride which will be captured by Cp_2TiCl^+ to afford Cp_2TiCl_2 as revealed by previous cyclic voltammetric studies.[15] In principle, these two processes might take place concertedly, which is the reason for showing the initial products within brackets. $Bn^\bullet$ is further reduced to the benzyl anion, Bn^-, in a fast second electron-transfer process (eq 12), and as this anion is expected to be a strong ligand we suggest that $Cp_2TiClBn$ is formed (possibly concertedly). The equivalent reactions of $(Cp_2TiCl)_2$ are depicted in eqs 13 and 14. Formally, the electron transfer from $(Cp_2TiCl)_2$ to BnCl in eq 13 would produce $(Cp_2TiCl)_2^+$, Cl^-, and $Bn^\bullet$ if it was not for the immediate follow-up reaction taking place between Cl^- and $(Cp_2TiCl)_2^+$. According to our previous cyclic voltammetric studies,[15] this reaction will afford Cp_2TiCl and Cp_2TiCl_2. The fast reduction of $Bn^\bullet$ by $(Cp_2TiCl)_2$ shown in eq 14 leads to the formation of Cp_2TiCl and $Cp_2TiClBn$. In the final step, eq 15, $Cp_2TiClBn$ produced in eqs 12 and 14 reacts in a relatively slow process with a second molecule of BnCl to afford Cp_2TiCl_2 and dibenzyl, Bn_2, as the final products in accordance with experimental observations (see the Experimental Section).

Analysis of the traces recorded was carried out on the basis of the above equations on the assumption that the reactions of eqs 12 and 14 would be so fast that their only influence on the kinetics would be through the reaction stoichiometry. The simulation program Gepasi 3.21 was employed,[25] giving a consistent set of data with the best fits depicted in Figure 9. Attempts to encompass a situation in the simulations, where the reactivity of the dimer would be negligible and the monomer with its free coordination site the only reactive species, lowered the quality of the fits. Furthermore, it was found that the equilibrium constant K_8 in that instance could hardly be larger than 30 M^{-1}, inconsistent with the value of $3 \times 10^3\ M^{-1}$ determined from the cyclic voltammetric measurements.[26]

In Table 2, we have collected the data extracted from the above measurements. As seen, the reactivity of Cp_2TiCl and $(Cp_2TiCl)_2$ is largely the same with $k_{11} = 0.66\ M^{-1}\ s^{-1}$ and $k_{13} = 0.80\ M^{-1}\ s^{-1}$, independent of the metal. A few kinetic experiments were carried out in the presence of 0.2 M Bu_4NPF_6 to have exactly the same experimental conditions as in the cyclic voltammetric experiments. It was found that while k_{11} was more than halved going to $0.30\ M^{-1}\ s^{-1}$, there was only a slight decrease in k_{13} to give $0.60\ M^{-1}\ s^{-1}$. From an electrostatic point of view, it would indeed be expected that the largest influence should be seen on the smallest species. Still, the effects are small considering that a lowering of the rate constant by a factor of 2.5 only corresponds to an increase in the activation energy of 0.5 kcal mol^{-1}. This also indicates that the charge separation in the transition state should be small.

The kinetic study of the cation Cp_2Ti^+ is much simpler since it can easily be generated without any interference from the other two Ti^{III} reagents by adding $TlPF_6$ to a solution of metal-free $Cp_2TiCl/(Cp_2TiCl)_2$ (see the Experimental Section). The mechanism for the reaction between Cp_2Ti^+ and BnCl is proposed to follow eqs 16−18.

$$Cp_2Ti^+ + BnCl \xrightarrow{k_{16}} [Cp_2Ti^{2+} + Cl^- + Bn^\bullet] \rightarrow Cp_2TiCl^+ + Bn^\bullet \quad (16)$$

$$Cp_2Ti^+ + Bn^\bullet \rightarrow [Cp_2Ti^{2+} + Bn^-] \rightarrow Cp_2TiBn^+ \quad (17)$$

$$Cp_2TiBn^+ + BnCl \rightarrow Cp_2TiCl^+ + Bn_2 \quad (18)$$

In the initial electron-transfer step (eq 16), $Bn^\bullet$ is formed along with chloride, which according to the cyclic voltammetric analysis will coordinate at the Ti^{IV} nucleus either concertedly or in an immediate follow-up reaction, thereby generating Cp_2TiCl^+. The benzyl radical is reduced by Cp_2Ti^+ in eq 17, affording Cp_2TiBn^+, which upon further reaction with BnCl (eq 18) will produce the final product Bn_2 along with Cp_2TiCl^+. The rate constant k_{16} can easily be determined to be $0.44\ M^{-1}\ s^{-1}$ under pseudo-first-order conditions as shown in Figure 10. This result is also included in Table 2.

A comparison of the reactivity of the different Ti^{III}-based species shows quite interestingly (see Table 2) that Cp_2Ti^+ exhibits almost the same reactivity as $(Cp_2TiCl)_2$ and Cp_2TiCl,

(25) Mendes, P. *Gepasi*, version 3.21; Virginia Tech: Blacksburg, VA, 1996−1999. The program may be downloaded via the Internet at http://www.gepasi.org.

(26) In cyclic voltammetry, Bu_4NPF_6 was used as the supporting electrolyte but the presence of this salt in the kinetic experiments did not improve the quality of the fits.

Table 2. Rate Constants k_{obs} for the Reaction between Ti^{III}−Based Species and Benzyl Chloride or Benzaldehyde Measured in THF at 20 °C along with Estimated Electron Transfer Rate Constants, k_{ET}, and k_{obs}/k_{ET} Ratios[a]

	BnCl			PhCHO		
	k_{obs}	k_{ET}	k_{obs}/k_{ET}	k_{obs}	k_{ET}	k_{obs}/k_{ET}
$Cp_2TiCl_2^-$[b]	<0.019	2.8×10^{-6}	$<6.8 \times 10^3$	<0.1	1.5×10^{-12}	$<6.7 \times 10^{10}$
$(Cp_2TiCl)_2$[c]	0.80	1.5×10^{-10}	5.3×10^9	70	1.2×10^{-28}	5.8×10^{29}
Cp_2TiCl[c]	0.66	4.2×10^{-11}	1.6×10^{10}	<2	4.7×10^{-31}	$<4.3 \times 10^{30}$
Cp_2Ti^+[d]	0.44	4.5×10^{-14}	9.8×10^{12}			

[a] All rate constants are given in units of $M^{-1}\ s^{-1}$; see text for description of the methods used for the determination of k_{ET}. [b] Generated electrochemically from Cp_2TiCl_2; a standard potential of −1.27 V vs Fc^+/Fc is employed in the calculation of k_{ET}; see ref 15. [c] Generated as a mixture of Cp_2TiCl and $(Cp_2TiCl)_2$ in Zn−Cp_2TiCl_2 solutions. [d] Generated as described in the text.

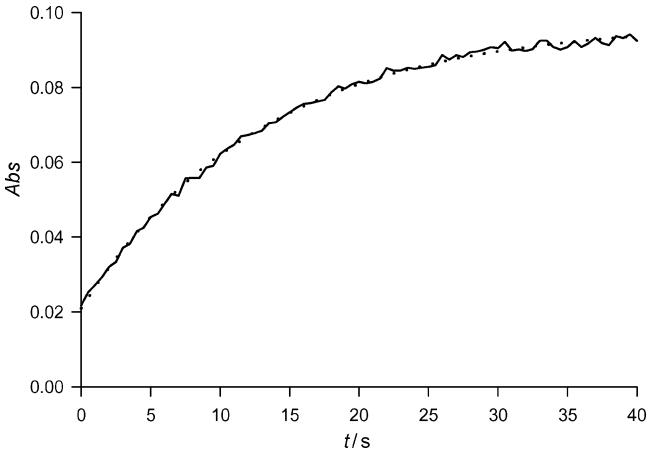

Figure 10. Kinetic trace recorded for the buildup of Ti^{IV} at $\lambda = 535$ nm in THF for the reaction of 87 mM BnCl with 0.5 mM Cp_2Ti^+. The dotted curve is the best exponential fit based on eqs 16−18, providing $k_{16} = 0.44\ M^{-1}\ s^{-1}$.

whereas $Cp_2TiCl_2^-$ is a much less efficient reagent. Presumably this can be explained by the fact that $Cp_2TiCl_2^-$ has no free coordination site so that a binding of the acceptor to the titanium nucleus cannot take place. This leads to an intrinsically slow reaction possessing very little inner-sphere electron-transfer character. On the other hand, for Cp_2Ti^+ and Cp_2TiCl easy replaceable solvent molecules will occupy the free ligand sites, facilitating a coordination of benzyl chloride during the reaction as illustrated by the structures **IV** and **V** in Chart 2. Note that within such structures chloride can readily be transferred as a ligand to the Ti^{IV} nucleus upon electron transfer.

In this sense, it is surprising that $(Cp_2TiCl)_2$, having no free coordination site in the assumed symmetric structure **II** (known from the solid phase, see Chart 1),[11] should exhibit the same reactivity as Cp_2TiCl. Previous stereochemical investigations have suggested that a pentavalent coordination is a possibility,[2a,i] but we think that a more plausible explanation could reside in the dimeric structure of $(Cp_2TiCl)_2$ being so weak that the same sort of coordination as suggested for Cp_2TiCl might take place during the electron transfer (see **VI**, Chart 2). There is even the possibility that the dimeric structure in THF from the very beginning is of the half-open type depicted as **III** in Chart 1, thereby leaving room for an easily accessible coordination site. Following the electron-transfer process and the transfer of chloride to the Ti^{IV} nucleus, the dimeric structure will be broken completely as outlined in eq 13. It is important to note that within this picture of concerted electron and ligand transfers the species given in the brackets of eqs 11−17 will not exist. Also investigated was whether the formation of any precursor complexes would be detectable in cyclic voltammetry. However, voltammograms of Zn−Cp_2TiCl_2 solutions recorded just after the addition of BnCl gave no such indications, nor did we see changes in the equilibrium ratio of Cp_2TiCl and $(Cp_2TiCl)_2$.

Benzaldehyde. A series of kinetic experiments was carried out on the reaction between Zn−Cp_2TiCl_2 (i.e., Cp_2TiCl and $(Cp_2TiCl)_2$) and PhCHO. This reaction is of great synthetic importance, as it presents a convenient route for accomplishing pinacol couplings.[2] The two other Ti^{III}-based species, Cp_2Ti^+ and $Cp_2TiCl_2^-$, were also included in this part of the study, although the measurements pertaining to Cp_2Ti^+ being irreproducible had to be renounced, and the reactivity of $Cp_2TiCl_2^-$ was found to be so low that only an upper limit of $0.1\ M^{-1}\ s^{-1}$ could be provided for the rate constant.

The reaction pathway in this case is assumed to consist of an initial electron transfer from Cp_2TiCl (eq 19) or $(Cp_2TiCl)_2$ (eq 20) to benzaldehyde, followed by dimerization of the thus formed ketyl radicals (eq 21).

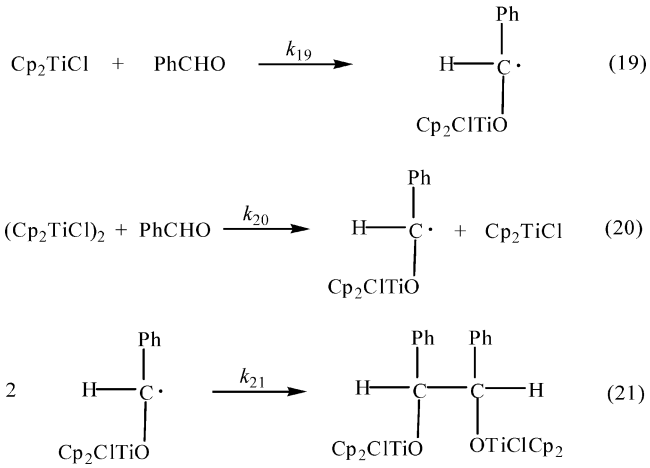

Note that the Ti^{IV} species formed upon electron transfer will be strongly coordinated at the oxygen and will not be liberated unless other strong electrophiles such as trimethylsilyl chloride or protons are added to the solution.[1f] Moreover, it is assumed that the dimeric structure of $(Cp_2TiCl)_2$ will be broken completely as the reaction in eq 20 progresses. In previous studies addressing the stereochemical outcome of pinacol couplings,[2] the possibility has been put forth that a pentavalent coordination involving two ketyl radicals can take place at the titanium nucleus in either the dimer **II**[2i] or the trinuclear complex **I**[2a,i] without the need to break bonds. Similar complexes have also been proposed, where two of the chlorides in **I** have been displaced by ketyl radicals.[1f,2c,d] The prominent feature of such arrangements is that they provide straightforward explanations for the high *dl*:*meso* ratios obtained. In contrast to this view stands the above cyclic voltammetric analysis pointing toward a rather fragile structure of the oxidized dimer ($k_{10} = 300\ s^{-1}$).

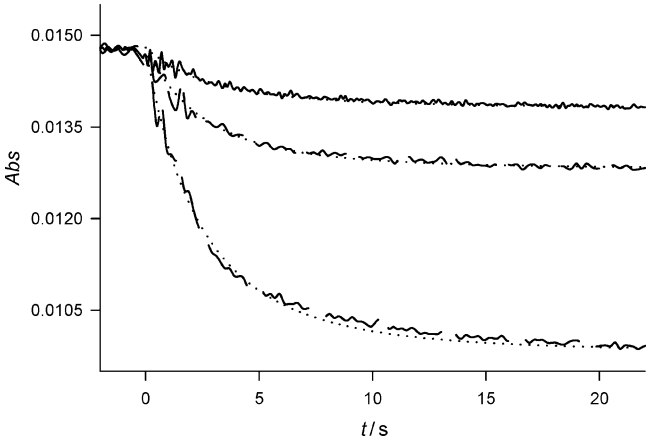

Figure 11. Kinetic traces recorded for the decay of Ti^{III} at $\lambda = 800$ nm in THF for the reactions of 15 mM PhCHO with 1 (—), 2 (– – –), and 5 mM (— — —) solutions of $Zn-Cp_2TiCl_2$. The initial absorption is set at 0.0148 in all three cases to facilitate comparison. The dotted curves are the best fits based on simulation of eqs 8 and 19−21, providing $k_{19} < 2$ M^{-1} s^{-1} and $k_{20} = 70$ M^{-1} s^{-1}.

Chart 2. Proposed Structures for the Coordination of Benzyl Chloride to Cp_2Ti^+ (**IV**), Cp_2TiCl (**V**) and $(Cp_2TiCl)_2$ (**VI**) and of Benzaldehyde to $(Cp_2TiCl)_2$ (**VII**) during the Electron Transfer Reactions

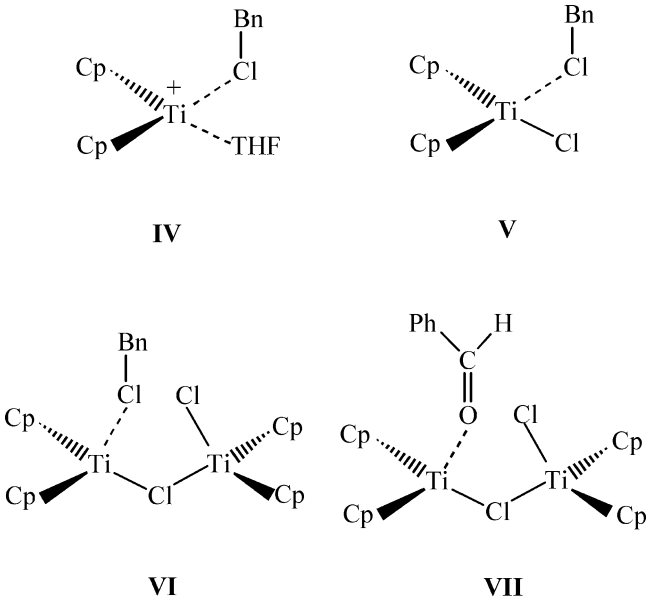

The fragmentation is even faster in the presence of a nucleophile such as chloride,[15] and there would be no reasons to expect that the ketyl radical should exert any weaker effect. Thus, kinetically there seem to be no arguments for the view that the dimeric structure should persist sufficiently long upon electron transfer to influence the dimerization step in eq 21.

The traces recorded for the overall decay of the Ti^{III} species for varying concentrations of $Zn-Cp_2TiCl_2$ in the presence of excess PhCHO are collected in Figure 11. This figure shows that the kinetics is not simple because the decay consists of a fast initial part followed by a long tail. The further analysis was based on the assumption that eq 8 and thus the equilibrium ratio of Cp_2TiCl and $(Cp_2TiCl)_2$ would be unaffected by the presence of PhCHO. This assumption seems reasonable on account of the observation that at least an aliphatic aldehyde such as propanal had no effect on the cyclic voltammetric response. The same type of measurements could not be carried out for PhCHO because of the fast reactions occurring in eqs 19−21. From the best fits included in Figure 11 it is found that $k_{19} < 2$ M^{-1} s^{-1} and $k_{20} = 70$ M^{-1} s^{-1}, thus showing that the influence from eq 19, in general, will be rather small.

The rate constants obtained are all included in Table 2. While the reactivity of $(Cp_2TiCl)_2$ and Cp_2TiCl in the case of benzyl chloride was found to be largely the same, this is certainly not the case for benzaldehyde, where the reactivity of $(Cp_2TiCl)_2$ surpasses that of Cp_2TiCl by at least a factor of 35. On this basis the arrangement of the dimer shown as **VII** in Chart 2, where one of the Ti^{III} atoms coordinates to the carbonyl group in benzaldehyde during the electron transfer, seems to present a plausible structure. Simulation of the reaction schemes for BnCl, eqs 8 and 11−15, and PhCHO, eqs 8 and 19−21 (with $k_{19} = 2$ M^{-1} s^{-1}), using the Gepasi program shows that in the case of a 100 mM $Zn-Cp_2TiCl_2$ solution (containing 100 mM of the substrates) 87.5 and 99.5%, respectively, will go through $(Cp_2TiCl)_2$. For a 0.5 mM solution, the corresponding percentages are 28.5 and 85.5%. The turnover points are reached at $Zn-Cp_2TiCl_2$ concentrations of 2.3×10^{-3} and 4.8×10^{-5} M for BnCl and PhCHO, respectively, on the assumption that the concentrations of the substrates are 100 mM. With respect to the product formation in the pinacol coupling reaction, it may thus be concluded that $(Cp_2TiCl)_2$ will be the species responsible, unless catalytic conditions are employed. On the other hand, this should have no implications for the *dl:meso* diastereoselectivities as the dimerization step in eq 21 is suggested to be the same for the two pathways involving Cp_2TiCl and $(Cp_2TiCl)_2$. This point will be further discussed in a forthcoming publication.[27]

The kinetic studies on the reactions with BnCl and PhCHO show that the reactivity order of the four principal Ti^{III} species is: $(Cp_2TiCl)_2 \gtrsim Cp_2TiCl \approx Cp_2Ti^+ \gg Cp_2TiCl_2^-$. From a thermodynamic point of view, it would be expected that $Cp_2TiCl_2^-$ with a 0.8 V lower oxidation potential than that of Cp_2Ti^+ should be the best electron donor. This indicates that at least the electron-transfer processes involving the three former species must be of the inner-sphere type. In this context, it is interesting to compare the extracted rate constants for the reaction between the different Ti^{III}-based species and BnCl or PhCHO, denoted generally k_{obs} (i.e., depending on the reaction considered it may correspond to k_{11}, k_{13}, k_{16}, k_{19}, or k_{20}), with those expected for electron-transfer reactions involving well-characterized electron donors such as aromatic radical anions. In the case of BnCl, the latter rate constants denoted k_{ET} may be deduced from the log k_{ET} vs E_A° plot shown in ref 24, where E_A° denotes the standard potential of the aromatic compound. Unfortunately, the same procedure for finding k_{ET} cannot be employed in the case of PhCHO, since the electron transfer from the aromatic radical anions to form the radical anion of benzaldehyde involves an energetically unfavorable equilibrium reaction. We therefore chose to calculate the required k_{ET} values between outer-sphere electron donors with E° values as listed in Table 1 and benzaldehyde on the basis of the equations of Marcus and Eyring.[28] The E° of benzaldehyde is −2.37 V vs Fc^+/Fc as measured by cyclic voltammetry, the reorganization

(27) Enemærke, R. J.; Larsen, J.; Hjøllund, G. H.; Skrydstrup, T.; Daasbjerg, K. Manuscript in preparation.
(28) Eberson, L. *Electron Transfer Reactions in Organic Chemistry* Springer-Verlag: Berlin, 1987.

energy of the reactions is assumed to be 10 kcal mol^{-1}, and for the collision frequency a value of 3×10^{11} M^{-1} s^{-1} is used.[28]

In Table 2, the k_{obs}/k_{ET} ratios are collected for BnCl and PhCHO with values ranging from less than 6.8×10^3 to 4.3×10^{30}. Usually, such large numbers would be indicative of substantial inner-sphere character of the transition state,[29] but in the present case one should exert great care in doing this kind of assessment, since a thorough analysis should also take into account differences in the reorganization energies, all relevant work terms, as well as the exact association constants for the formation of precursor complexes.[24] One could easily imagine that the latter would be of particular importance for the reactions of PhCHO. In addition, the finding of relatively small heterogeneous rate constants in Table 1 indicates that the reorganization energy for the Ti^{III} species is substantially larger than that for aromatic radical anions. At the present stage, we therefore prefer to develop a relative scale of uncorrected k_{obs}/k_{ET} ratios, which are still very useful for carrying out comparisons, rather than paying further attention at the absolute values.

For both BnCl and PhCHO, the k_{obs}/k_{ET} ratios decrease in the order Cp_2Ti^+, Cp_2TiCl, $(Cp_2TiCl)_2$, and $Cp_2TiCl_2^-$. This would imply that there should be substantially more inner-sphere character in the reactions of Cp_2Ti^+ than those of Cp_2TiCl, $(Cp_2TiCl)_2$, and in particular $Cp_2TiCl_2^-$. In fact, this is in line with expectations since the cation Cp_2Ti^+ compared with the anion $Cp_2TiCl_2^-$ would be expected to have a stronger coordination in the transition state to the developing Cl^- in BnCl and O^- in PhCHO. From both a kinetic and thermodynamic point of view, the features of $Cp_2TiCl_2^-$ ($E^\circ = -1.27$ V vs Fc^+/Fc; $k_{obs} < 0.019$ M^{-1} s^{-1} and $k_{obs}/k_{ET} < 6.8 \times 10^3$ for BnCl) are comparable with those of SmI_2 ($E^\circ = -1.41$ V vs Fc^+/Fc; $k_{obs} = 0.02$ M^{-1} s^{-1} and $k_{obs}/k_{ET} = 250$ for BnCl),[24] although it is hard to carry out a direct comparison of the k_{obs}/k_{ET} ratios for the reasons given above. Finally, it may be concluded that the inner-sphere character of the processes involving PhCHO is stronger than for BnCl and that this feature is getting more pronounced as the thermodynamic electron-donating abilities of the Ti^{III} complex are lowered.

Experimental Section

Materials. Most chemicals were of commercial origin unless otherwise noted. Benzyl chloride and benzaldehyde were vacuum distilled before use. THF was distilled over sodium and benzophenone under an atmosphere of dry nitrogen. Argon (99.99% purity) was passed through a column of P_2O_5 (Sicapent). Tetrabutylammonium hexafluorophosphate, Bu_4NPF_6, was prepared from a hot aqueous solution containing tetrabutylammonium hydrogen sulfate and potassium hexafluorophosphate. The precipitate was filtered and recrystallized from ethyl acetate and pentane. Tetrabutylammonium chloride, Bu_4NCl, was recrystallized twice using THF. The white crystals were dried under vacuum at 60 °C for 24 h and stored in a glovebox. All handling of Bu_4NCl had to occur in a dry atmosphere because of its hygroscopic properties. Thallium hexafluorophosphate, $TlPF_6$, was dried under vacuum at 60 °C for 24 h. Thallium cyclopentandienide, TlCp, was sublimated under vacuum at 80 °C.[30] Bis(cyclopentadienyl)titanium dichloride, Cp_2TiCl_2, was recrystallized from toluene. The metal-free solution of $Cp_2TiCl/(Cp_2TiCl)_2$ was synthesized as described previously.[10] Typically, $TiCl_3$ was suspended in THF and added to a solution containing 2 equiv of TlCp. While the solution was refluxed for 15 min it turned green, and a precipitation of TlCl occurred. The separation was carried out using syringe techniques. The Zn− and Mn−Cp_2TiCl_2 solutions were prepared by adding THF to a flask thoroughly flushed with argon and containing Cp_2TiCl_2 besides excess metal. The solutions were stirred for 30 min until a turquoise green color had become apparent. For preparing Al−Cp_2TiCl_2, activation of the aluminum foil using $Hg(NO_3)_2$ in THF was required. The activated foil was washed three times with THF before use. The preparation of Cp_2TiPF_6 was accomplished by adding 1.1 equiv of $TlPF_6$ dissolved in THF to a metal-free solution of $Cp_2TiCl/(Cp_2TiCl)_2$. The mixture was stirred and heated shortly to the boiling point; blue crystals of Cp_2TiPF_6 along with white crystals of TlCl then precipitated. The liquid was removed, and the crystals were washed twice with THF. A large amount of THF was subsequently added, and after 30 min of stirring the solution turned pale blue. The concentration of Cp_2TiPF_6 in this saturated solution was approximately 2 mM as determined from peak current measurements.[31]

Apparatus. Most of the electrochemical equipment was home-built, and a description of the experimental setup is provided in ref 32. The working electrode was a glassy carbon disk of diameter 1 mm. The electrode surface was polished using 0.25 μm diamond paste (Struers A/S), followed by cleaning in an ethanol bath. The counter electrode consisted of a platinum coil melted into glass, while a silver wire in a sintered glass containing THF/0.2 M Bu_4NPF_6 + 0.02 M Bu_4NI served as the reference electrode. All potentials were reported against the ferrocenium/ferrocene (Fc^+/Fc) redox couple, the potential of which has been measured to be 0.52 V vs SCE in THF/0.2 M Bu_4NPF_6.[23] All handling of chemicals was performed on a vacuum line, and at no point during the different operations was the interference of oxygen allowed. The ohmic drop was compensated with a positive feedback system incorporated in the potentiostat. The kinetic traces were recorded by means of a fiber-optic spectrometer, model S1000 (dip-probe), from Ocean Optics, using a light path length of 1 cm.

Procedure. In the cyclic voltammetric experiments, 0.77 g of Bu_4NPF_6 (2.0 mmol) and a small magnetic bar were added to the electrochemical cell. The cell was closed and flushed thoroughly with argon for 10 min. Typically, 9 mL of freshly distilled THF and 1 mL of the appropriate standard solution containing the compound of interest were added to the cell using a syringe, and the solution was stirred for 30 s. Special care must be taken when recording voltammograms of the Met−Cp_2TiCl_2 solutions, since the metal ions present may be reduced at low potentials and cause deleterious adsorption of metal on the electrode surface. In general, potentials below −1.3 V vs Fc^+/Fc should be avoided. At the end of each series of experiments a small amount of ferrocene was added, and the potential of the Fc^+/Fc couple was measured.

In the kinetic experiments, the UV−vis dip-probe was mounted vertically in a two-necked cell containing a small magnetic bar.[32] The cell was closed and flushed with argon for 10 min before 9 mL of freshly distilled THF was added. From a standard solution containing the appropriate Met−Cp_2TiCl_2, typically 1 mL was transferred to the cell. Benzyl chloride or benzaldehyde was added in excess, while the solution was stirred vigorously. The decay of Ti^{III} at the wavelength $\lambda = 800$ nm and the concomitant buildup of Ti^{IV} at $\lambda = 535$ nm were followed. Analysis of the products formed in the reaction of Zn−Cp_2TiCl_2 with benzyl chloride showed (after acidic quenching) formation of both dibenzyl and toluene, the ratio of which increased as the reaction time was prolonged. This indicates that the reaction shown in eq 15 is relatively slow occurring in the time scale of hours.

Conclusions

Detailed cyclic voltammetric studies of Zn-, Mn-, and Al-reduced Cp_2TiCl_2 solutions in THF show that the principal

(29) Lund, H.; Daasbjerg, K.; Lund, T.; Pedersen, S. U. *Acc. Chem. Res.* **1995**, *28*, 313.
(30) Nielson, A. J.; Rickard, C. E. F.; Smith, J. M. *Inorg. Synth.* **1990**, *28*, 315.
(31) Bard, A. J.; Faulkner, R. *Electrochemical Methods, Fundamentals and Applications*; Wiley: New York, 1980.
(32) Pedersen, S. U.; Christensen, T. B.; Thomasen, T.; Daasbjerg, K. *J. Electroanal. Chem.* **1998**, *454*, 123.

Ti^{III} species present are a mixture of Cp_2TiCl and $(Cp_2TiCl)_2$, independent of the metal considered; the equilibrium constant of dimerization is determined to be $3 \times 10^3\ M^{-1}$. There are no indications of trinuclear complexes or ionic clusters involving Cp_2Ti^+ as suggested previously. Nor do we see the formation of $Cp_2TiCl_2^-$ as found in the electrochemical reduction of Cp_2TiCl_2, because chloride now becomes firmly bound by the corresponding metal chlorides. According to the standard potentials determined in cyclic voltammetry the electron-donating ability of the different Ti^{III}-based species would be expected to be in the order $Cp_2TiCl_2^- \gg (Cp_2TiCl)_2 > Cp_2TiCl \gg Cp_2Ti^+$. However, in reality the reactivity order is $(Cp_2TiCl)_2 \gtrsim Cp_2TiCl \approx Cp_2Ti^+ \gg Cp_2TiCl_2^-$, as assessed in their reactions with benzyl chloride and benzaldehyde. In general, it is found that $(Cp_2TiCl)_2$ will be the species responsible for the product formation, unless catalytic conditions characterized by low concentrations of Ti^{III} are employed. None of the reactions studied in this article proceed by an outer-sphere electron-transfer pathway, and the inner-sphere character of the reactions of Cp_2Ti^+ is clearly much higher than those of $(Cp_2TiCl)_2$, Cp_2TiCl, and in particular $Cp_2TiCl_2^-$. As for the electron acceptor, the inner-sphere character of the transition state increases going from benzyl chloride to benzaldehyde, and it is suggested that Cl in benzyl chloride and O in benzaldehyde could function as bridges between the reactants in the transition state. In a forthcoming publication[27] the focus will be on metal-reduced solutions of Cp_2TiBr_2 and Cp_2TiI_2 as well as the factors influencing the reactivities and diastereoselectivities of the pinacol coupling reaction involving benzaldehyde.

Acknowledgment. Torben Bo Christensen is thanked for diligent technical assistance.

Supporting Information Available: Text giving a description of the model parameters used in the simulations and figures giving a compilation of relevant fits (PDF). This material is available free of charge via the Internet at http://pubs.acs.org.

JA0491230